PCCP

COMMUNICATION

View Article Online
View Journal | View Issue

Cite this: *Phys. Chem. Chem. Phys.*, 2024, **26**, 23566

Received 2nd August 2024,
Accepted 2nd September 2024

DOI: 10.1039/d4cp03070b

rsc.li/pccp

NIR-triggered upconversion and sensitized NIR-emission in Yb-based Eosin Y lake doped latex nanoparticles†

Rita B. Cevallos-Toledo, Delia Bellezza, María González-Béjar * and Julia Pérez-Prieto *

Here, Yb-based Eosin Y lakes (EOS-Yb) have been encapsulated in organic nanoparticles (NPs) by microemulsion radical polymerization of methacrylate-based copolymers. These photoactive EOS-Yb NPs emit in the visible and near infrared (NIR) upon excitation at 530 nm and can also display NIR-to-visible upconversion emission upon excitation at 980 nm.

Photoactive materials with absorption and emission in the NIR region are commonly used in applications such as bio-imaging, LEDs and for luminescent probes.[1] Ytterbium (Yb^{3+}) absorbs in the NIR and has a single excited state with emission in the NIR. In this context, materials containing a photoactive lanthanide (Ln) can absorb at different wavelengths and convert them to different emissions (*e.g.*, UVA/visible-to-NIR, NIR-to-NIR or NIR-to-visible) depending on their configuration.[2] Upconversion (UC) refers to optical processes that convert photons absorbed at longer wavelengths to shorter ones.[3]

Many Ln-based materials present the so called antenna effect (AE).[4] This refers to the photosensitization of the Ln by an excited organic chromophore.[5] Furthermore, Ln-based materials[6] (*e.g.*, Ln-complexes) also present interesting features such as: (i) strong and sharp luminescence, (ii) large Stokes or anti-Stokes shifts, (iii) long luminescence lifetimes, (iv) thermal stability and (v) photostability.[7,8]

Upon light excitation, certain Ln-based materials can engage in different UC mechanisms.[9] In particular, cooperative sensitization (CS) occurs when two close lying lanthanide ions reach a virtual state and subsequently transfer the energy to another photoactive moiety (whether it be a lanthanide ion or an organic molecule), eventually leading to the final emission (*e.g.*, complexes containing $[Yb_2Tb]$,[10] $[Gd_7Tb_2Yb_7]$,[11] $RuYb_3$[12] or Yb-based Eosin Y lakes ($[EOS]_x[Yb]_x$)[13]).

Scheme 1 displays the possible photophysical mechanisms that could take place upon visible or NIR excitation of Yb-based Eosin Y lakes. Remarkably, CS is not sensitive to oxygen as opposed to triplet–triplet annihilation (TTA) upconversion.[14]

Polymer encapsulated nanoparticles containing emissive dyes, upconversion NPs or luminescent conjugated porous polymers have been extensively studied.[15–18] Organic polymeric NPs have also been used to encapsulate Ln-complexes, that displayed an antenna effect, thus avoiding deactivation, while improving their processability and biocompatibility.[18]

Polystyrene (PS) is commonly used to encapsulate emissive Ln-complexes, as the single polymer[19,20] or with other copolymers such as polyethylene glycol (PEG),[21] polyacrylic acid (AAc)[22] or maleic acid (MA).[23] Other polymers such as poly(9-vinylcarbazole),[24] poly(sodium 4-styrenesulfonate) (PSS)[25] and polymethyl methacrylate (PMMA)[26–28] have also been used. Their photophysical features and NP sizes are summarized in Table S1 (ESI†). Although some of them contained NIR-emissive Ln, only one of them[22] was evaluated for UC.[18,25]

EOS-Yb is soluble in DMF and DMSO but not in water. Encapsulating EOS-Yb into NPs would prevent EOS-Yb precipitation in

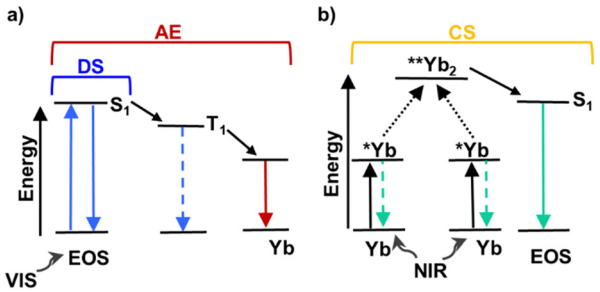

Scheme 1 (a) Downshifting (DS) luminescence and antenna effect (AE) can occur upon visible excitation of Yb-based Eosin Y lakes. (b) Cooperative sensitization (CS) of Yb in Yb-based Eosin Y lakes upon NIR excitation. Note: dashed lines represent non-radiative deactivation.

Instituto de Ciencia Molecular (ICMol), Universitat de València, Catedrático José Beltrán 2, Paterna, 46980 Valencia, Spain. E-mail: julia.perez@uv.es, maria.gonzalez@uv.es

† Electronic supplementary information (ESI) available. See DOI: https://doi.org/10.1039/d4cp03070b

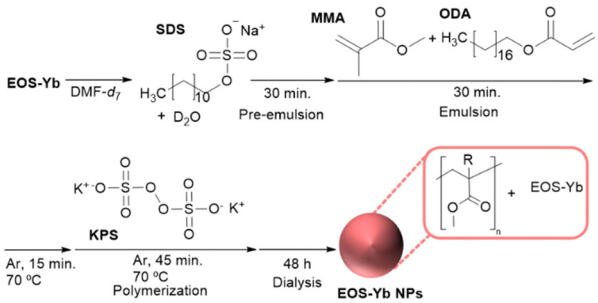

Scheme 2 Synthesis and purification of EOS-Yb NPs carried out in darkness.

water. Indeed, the surface of the nanoparticles could be easily modified for subsequent targeting if required.

Previously, our group has reported the synthesis of an Yb-based Eosin Y lake material (EOS-Yb)[13] that exhibits CS upconversion upon NIR excitation at 980 nm, with emission centred at 600 nm. We envisaged that photoactive NPs, able to undergo up and down energy transfer processes, could be designed by encapsulating EOS-Yb within an organic polymer.

Building on a protocol previously used for Ln-complexes, we have successfully encapsulated EOS-Yb in polymeric NPs by using methacrylate-based copolymers. The NIR-luminescence upon visible excitation together with their NIR-triggered UC properties of EOS-Yb are here described. EOS-Yb nanoparticles (EOS-Yb NPs) were prepared by microemulsion polymerization[28] with some modifications (Scheme 2). The monomer is pre-organized into nanodroplets that act as independent nanoreactors, and allow to dissolve the organo-Ln complex in the monomer before initiating the polymerization.[29]

Briefly, 40 mg of EOS-Yb were dissolved in 600 μL of deuterated *N*,*N*-dimethylformamide (DMF-d_7).‡ Then, sodium dodecylsulfate (SDS; 0.3 mmol) dissolved in D_2O was added. The mixture was vigorously stirred for 30 min. Next, octadecyl acrylate (ODA; 0.6 mmol) was mixed with methyl methacrylate (MMA; 46.9 mmol). The monomers were added to the previous mixture, and then vigorously stirred for 30 min to homogenize the mixture. This microemulsion was transferred to a two neck round bottom flask equipped with a condenser, degassed with Ar and heated to 70 °C under stirring for 15 min. Subsequently, potassium persulfate (KPS; 0.4 mmol), previously dissolved in 2.5 mL of D_2O, was added to initiate the free radical polymerization under Ar; polymerization continued for 45 min. Then, the mixture was purified by dialysis against milliQ water for 48h with a membrane of regenerated cellulose of 3.5KDa. The synthesis and purification of the as-prepared NPs were carried out in darkness because EOS-Yb photobleached under laboratory light before encapsulation under these experimental conditions. Remarkably, the purified EOS-Yb NPs aqueous dispersion remained dispersed and photostable after storage for 8 months under laboratory light.

The EOS-Yb NPs are spherical, with an average size of 50 nm ± 0.4 nm as measured by scanning electron microscopy (SEM) (Fig. 1a); the size histogram is shown in Fig. 1b.

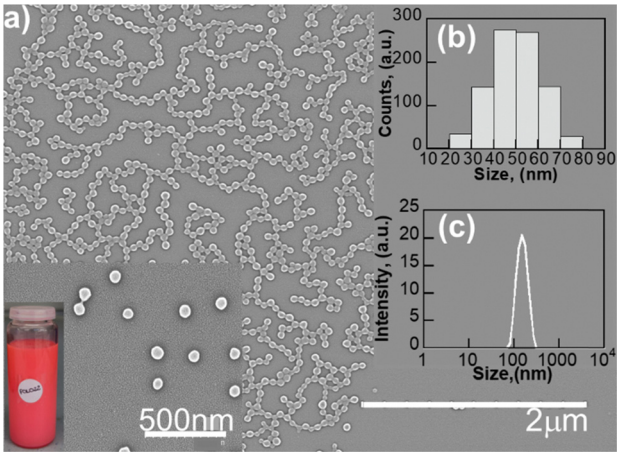

Fig. 1 (a) SEM image (b) histogram and (c) DLS average histogram of EOS-Yb NPs. Inset: Magnification of the SEM image with a photograph of EOS-Yb NPs under laboratory light.

The hydrodynamic diameter of the NPs was 118 ± 0.4 nm as measured by dynamic light scattering (DLS) (Fig. 1c) in DMSO with a polydispersity index (PDI) of 0.1.

Ultrasonication at the emulsion step was used under different conditions (time, amplitude, and pulse/pause sequence) but led to similar results. Attempts to obtain NPs by either starting from higher loadings of EOS-Yb, or by dissolving EOS-Yb in a mixture of MMA and ODA, did not result in any increase on the amount of EOS-Yb encapsulated into the polymeric NPs or different size distributions.

Other fruitless attempts for EOS-Yb encapsulation were performed, such as nanoprecipitation with 1,6-hexanediol; synthesis of reverse micelles in DMSO (EOS-Yb has low solubility in other solvents) with two different surfactants (dioctyl sulfosuccinate sodium salt and SDS), and PEG encapsulation.

Inductively coupled plasma mass spectrometry (ICP-MS) revealed that *ca.* 83% of the starting Yb was encapsulated. This corresponds to 0.7 wt% relative to the monomers. This is consistent with the limited quantity of Ln-complex (*ca.* 2 wt%) that can be loaded within the latex NPs.[28]

For comparative purposes, a similar synthesis was carried out to encapsulate Eosin Y (EOS); thus, obtaining EOS NPs. They present spherical shape with a hydrodynamic diameter of 107 ± 0.8 nm and a PDI of 0.05 (Fig. S1, ESI†).

X-ray photoelectron spectroscopy (XPS) of C 1s, O 1s, Br 3d and Yb 4d of EOS-Yb NPs and EOS NPs was carried out (see Fig. S2, ESI†).

In both EOS-Yb NPs and EOS NPs the C 1s and O 1s spectra resemble to the XPS spectra of PMMA. The band at 532 eV (C═O) and the one at 533.5 eV (C–O) are shifted to higher binding energies than in PMMA, 0.7 and 1eV respectively.[30]

The Br 3d spectra of EOS-Yb NPs and EOS NPs are very similar, but new bands appear at higher binding energies for EOS-Yb, which can be assigned to the Br coordinated to Yb.[31]

The typical absorption and emission spectra of EOS were observed upon excitation at 530 nm of colloidal dispersions of EOS-Yb NPs in DMSO-d_6 under air (Fig. 2). The EOS-Yb NPs

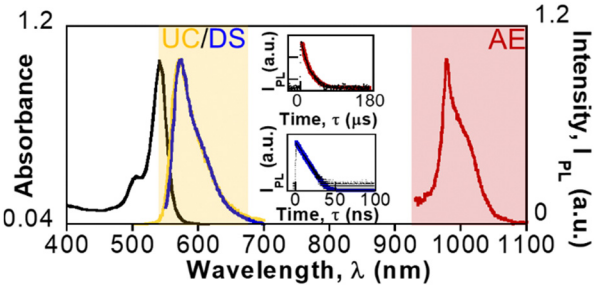

Fig. 2 Optical properties of EOS-Yb NPs: Absorption spectrum (black line). Downshifting (blue line) and antenna effect (red line); λ_{ex} = 530 nm. Upconversion emission (yellow line); (λ_{ex} = 980 nm). Inset: Kinetic traces at λ_{ex} = 530 nm and λ_{em} = 980 nm (top) and λ_{ex} = 530 nm and λ_{em} = 574 nm (bottom). All measurements were carried out in DMSO-d_6.

downshifting (DS) emission is centered at 574 nm with a lifetime of 5.11 ns (Fig. 2 inset) and a quantum yield (QY) of 0.85.

Given the fact that EOS-Yb NPs contain an organic chromophore (EOS) and a lanthanide (Yb), when EOS was excited at 530 nm, Yb emitted at 980 nm due to the antenna effect (Fig. 2) with a lifetime of 8.8 μs (Fig. 2 inset). The Stokes shift was 406 nm. Comparatively, the DS emission of EOS-Yb NPs (λ_{ex} = 530 nm) was 30% higher than that of EOS NPs (Fig. S3, ESI†). As expected, EOS NPs did not emit in the NIR region due to the absence of Yb.

As expected, EOS-Yb NPs also showed UC emission centered at 574 nm upon NIR excitation at 980 nm, which corresponds to an anti-Stokes shift of 448 nm. The UC emission was 20% higher for EOS-Yb NPs than for EOS NPs (Fig. S4, ESI†), even if EOS had similar absorption. Usually, the maximum emission wavelength of EOS is red-shifted at higher concentrations.[32] The UC emission of EOS NP could be attributed to two-photon absorption.

The maximum of UC emission of EOS-Yb NPs was slightly blue-shifted (574 nm), as compared to that of EOS NPs (576 nm); this is consistent with the low concentration of EOS-Yb inside the NPs (Fig. S5, ESI†). This concentration was too low to measure the photoluminescence QY or the UC lifetime. In our previous work, an increase of EOS-Yb concentration led to an enhancement of the UC emission.[13]

The effect of the atmosphere (air and Ar) in the UC process was also evaluated to distinguish if the mechanism occurs *via* CS or TTA. There was a negligible difference for EOS-Yb NPs, (Fig. 3a), implying that the UC mechanism is consistent with CS.

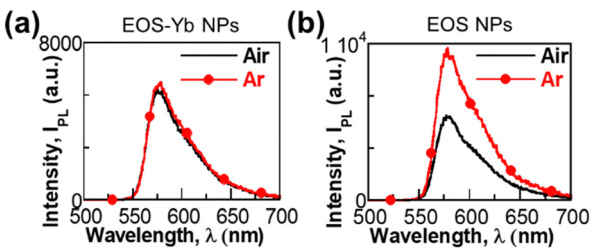

Fig. 3 Effect of oxygen on the UC emission (λ_{ex} = 980 nm) of (a) EOS-Yb NPs and (b) EOS NPs in DMSO-d_6.

Conversely, when the EOS NPs were excited at 980 nm under Ar, the emission intensity increased by 56% as compared to the aerated sample (Fig. 3b), indicating that the triplet state is involved in the emission mechanism in this case (TTA has been previously reported for xanthenic dyes).[33]

The CS mechanism is supported by the log–log plot of the emission (λ_{ex} = 980 nm) of EOS-Yb NPs *versus* laser power density. It shows a straight line with a slope of *ca.* two. This indicates that two photons are required to achieve the UC process, mirroring the behaviour observed in the EOS-Yb lake (Fig. S6, ESI†).[13]

Conclusions

Latex NPs have been doped with Yb-based Eosin Y lakes (EOS-Yb). The use of EOS-Yb with EOS and Yb allows either for excitation in the visible, thereby leading to EOS downshifting and Yb sensitization (antenna effect) or for NIR excitation leading to upconversion emission (not sensitive to air). Even if EOS-Yb NPs did not present the same upconversion intensity as the EOS-Yb material, these NPs are easier to process and dispersible in solvents such as DMSO and water as opposed to EOS-Yb. EOS-Yb NPs could be tested in the future for biological applications.

Author contributions

R. B. Cevallos-Toledo investigation, methodology, data curation, visualization, formal analysis, writing – original draft. D. Bellezza investigation. M. González-Béjar: conceptualization, funding acquisition, project administration, methodology, supervision, writing – original draft; writing – review & editing; Julia Pérez-Prieto: conceptualization, funding acquisition, project administration, supervision, writing – review & editing.

Data availability

The data supporting this article have been included as part of the ESI.†

Conflicts of interest

There are no conflicts to declare.

Acknowledgements

This research was funded by MINECO; Agencia Estatal de Investigación-AEI (grant number MCIU Unit of Excellence "Maria de Maeztu" CEX2019-000919-M), Generalitat Valenciana (GVA) (IDIFEDER/2018/064, IDIFEDER/2021/064, CIPROM/2022/57 and GRISOLIA/2019/041 to R.-B. C.), all of them partially cofinanced with FEDER funds and Conselleria d'Educació, Universitats i Ocupació This study forms part of the Advanced Materials programme (MFA/2022/051) and was supported by MICIN with funding from European Union NextGenerationEU (PRTR-C17.I1) and by GVA.

Notes and references

‡ Deuterated solvents were used in the synthesis to avoid quenching of the excited state of Yb due to the vibrations of the C–H, N–H or O–H bonds in the solvent.

1 D. A. Gálico, C. M. Santos Calado and M. Murugesu, *Chem. Sci.*, 2023, **14**, 5827–5841.
2 K. Binnemans, *Chem. Rev.*, 2009, **109**, 4283–4374.
3 F. Auzel, *Chem. Rev.*, 2004, **104**, 139–173.
4 S. I. Weissman, *J. Chem. Phys.*, 1942, **10**, 214–217.
5 A. D'Aléo, F. Pointillart, L. Ouahab, C. Andraud and O. Maury, *Coord. Chem. Rev.*, 2012, **256**, 1604–1620.
6 G. A. Crosby, R. E. Whan and R. M. Alire, *J. Chem. Phys.*, 1961, **34**, 743–748.
7 S. Dasari, S. Singh, P. Kumar, S. Sivakumar and A. K. Patra, *Eur. J. Med. Chem.*, 2019, **163**, 546–559.
8 J. Feng and H. Zhang, *Chem. Soc. Rev.*, 2013, **42**, 387–410.
9 L. J. Charbonnière, A. M. Nonat, R. C. Knighton and L. Godec, *Chem. Sci.*, 2024, **15**, 3048–3059.
10 N. Souri, P. Tian, C. Platas-Iglesias, K.-L. Wong, A. Nonat and L. J. Charbonnière, *J. Am. Chem. Soc.*, 2017, **139**, 1456–1459.
11 D. A. Gálico and M. Murugesu, *Angew. Chem., Int. Ed.*, 2022, **61**, 1–8.
12 R. C. Knighton, L. K. Soro, L. Francés-Soriano, A. Rodríguez-Rodríguez, G. Pilet, M. Lenertz, C. Platas-Iglesias, N. Hildebrandt and L. J. Charbonnière, *Angew. Chem., Int. Ed.*, 2022, **61**, 1–7.
13 R. B. Cevallos-Toledo, D. Bellezza, J. Ferrera-González, A. Giussani, E. Ortí, M. González-Béjar and J. Pérez-Prieto, *ChemPhotoChem*, 2023, **7**, 1–7.
14 N. Kiseleva, P. Nazari, C. Dee, D. Busko, B. S. Richards, M. Seitz, I. A. Howard and A. Turshatov, *J. Phys. Chem. Lett.*, 2020, **11**, 2477–2481.
15 K. Li and B. Liu, *Chem. Soc. Rev.*, 2014, **43**, 6570–6597.
16 T. Vasylyshyn, V. Patsula, M. Filipová, R. L. Konefal and D. Horák, *Nanoscale Adv.*, 2023, **5**, 6979–6989.
17 D. Mendez-Gonzalez, V. Torres Vera, I. Zabala Gutierrez, C. Gerke, C. Cascales, J. Rubio-Retama, O. G. Calderón, S. Melle and M. Laurenti, *Small*, 2022, **18**, 1–14.
18 C. Cheignon, A. A. Kassir, L. K. Soro and L. J. Charbonnière, *Nanoscale*, 2022, **14**, 13915–13949.
19 K. Tamaki, H. Yabu, T. Isoshima, M. Hara and M. Shimomura, *Colloids Surf., A*, 2006, **284–285**, 355–358.
20 J. Desbiens, B. Bergeron, M. Patry and A. M. Ritcey, *J. Colloid Interface Sci.*, 2012, **376**, 12–19.
21 K. Tamaki and M. Shimomura, *Int. J. Nanosci.*, 2002, **01**, 533–537.
22 P. Huhtinen, M. Kivela, O. Kuronen, V. Hagren, H. Takalo, H. Tenhu and H. Ha, *Anal. Chem.*, 2005, **77**, 2643–2648.
23 W. Yang, L. M. Fu, X. Wen, Y. Liu, Y. Tian, Y. C. Liu, R. C. Han, Z. Y. Gao, T. E. Wang, Y. L. Sha, Y. Q. Jiang, Y. Wang and J. P. Zhang, *Biomaterials*, 2016, **100**, 152–161.
24 W. Sun, J. Yu, R. Deng, Y. Rong, B. Fujimoto, C. Wu, H. Zhang and D. T. Chiu, *Angew. Chem., Int. Ed.*, 2013, **52**, 11294–11297.
25 R. R. Zairov, A. P. Dovzhenko, A. S. Sapunova, A. D. Voloshina, D. A. Tatarinov, I. R. Nizameev, A. T. Gubaidullin, K. A. Petrov, F. Enrichi, A. Vomiero and A. R. Mustafina, *Mater. Sci. Eng., C*, 2019, **105**, 1–10.
26 M. Cardoso Dos Santos, A. Runser, H. Bartenlian, A. M. Nonat, L. J. Charbonnière, A. S. Klymchenko, N. Hildebrandt and A. Reisch, *Chem. Mater.*, 2019, **31**, 4034–4041.
27 G. Shao, R. Han, Y. Ma, M. Tang, F. Xue, Y. Sha and Y. Wang, *Chem. – Eur. J.*, 2010, **16**, 8647–8651.
28 N. Wartenberg, O. Raccurt, D. Imbert, M. Mazzanti and E. Bourgeat-Lami, *J. Mater. Chem. C*, 2013, **1**, 2061–2068.
29 R. Muñoz-Espí, C. K. Weiss and K. Landfester, *Curr. Opin. Colloid Interface Sci.*, 2012, **17**, 212–224.
30 X. L. Zhu, S. B. Liu, B. Y. Man, C. Q. Xie, D. P. Chen, D. Q. Wang, T. C. Ye and M. Liu, *Appl. Surf. Sci.*, 2007, **253**, 3122–3126.
31 B. Li, Y. Zhang, F. Duanmu, Y. Shen, Z. Shen and S. Zhong, *Photochem. Photobiol. Sci.*, 2019, **18**, 1408–1418.
32 S. De, S. Das and A. Girigoswami, *Spectrochim. Acta - Part A Mol. Biomol. Spectrosc.*, 2005, **61**, 1821–1833.
33 A. Kumar, L. Pinto da Silva, J. C. G. Esteves da Silva and K. Kumar, *Opt. Mater.*, 2019, **96**, 109286.